THE JOURNAL OF PHYSICAL CHEMISTRY B

Article

pubs.acs.org/JPCB

Nanoscale Chains Control the Solubility of Phosphate Glasses for Biomedical Applications

Jamieson K. Christie,* Richard I. Ainsworth, Devis Di Tommaso, and Nora H. de Leeuw

Department of Chemistry, University College London, 20 Gordon Street, London, WC1H 0AJ, U.K.

ABSTRACT: Bioactive phosphate-based glasses (PBGs) have several possible biomedical applications because of the chemical reactions they undergo with their surroundings when implanted into the body. The dissolution rate of PBGs in physiological conditions is a crucial parameter for these applications, to ensure, e.g., delivery of drugs or nutrients to the body at the correct rate. While it has been well-known that increasing the CaO content of these glasses at the expense of Na_2O slows the dissolution rate, this paper provides an atomistic explanation of this for the first time. In this work, molecular dynamics simulations of five ternary P_2O_5−CaO−Na_2O glasses reveal the structural properties at the atomic level that enhance the durability of PBGs as more Ca is added: (i) Ca binds together more fragments of the phosphate glass network than Na, (ii) Ca binds together more PO_4 tetrahedra than Na, and (iii) Ca has a lower concentration of intratetrahedral phosphate bonding than Na. This behavior is rooted in the calcium ion's higher charge and field strength. These results open the path to precise control and optimization of the PBG dissolution rate for specific biomedical applications.

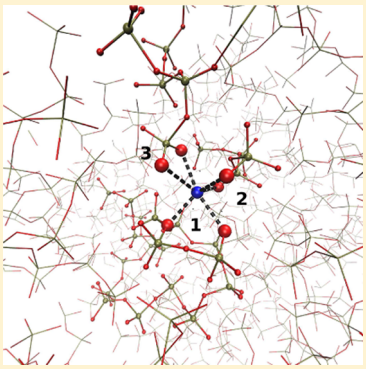

INTRODUCTION

Ternary phosphate glasses, containing phosphorus, sodium, calcium, and oxygen, are bioactive; i.e., they react chemically when placed in a physiological environment. As a result, they have substantial applications in biomedicine,[1] including in neural repair,[2] tissue engineering,[3] and bone fracture fixation[4] and as delivery devices for the controlled release of drugs, nutrients, or antimicrobials.[5,6]

Ternary phosphate-based bioactive glasses (PBGs) have a composition-dependent dissolution rate in physiological media, which can vary over several orders of magnitude.[3,7] For example, when the glass contains approximately 50 mol % P_2O_5 (metaphosphate composition), several studies[3,4,7−9] show that increasing the concentration of CaO at the expense of Na_2O leads to a dramatic decrease in the glass dissolution rate, although we do not have an atom-level explanation of this phenomenon. Control of the dissolution rate is vital in tissue engineering; degradable biomaterials are the materials of choice where the dissolution products have an active role, whereas substances involved in targeted controlled delivery need to be released at the appropriate rate, and sutures or temporary bone fixation need to dissolve over the correct time scale to ensure their successful use. However, there is little molecular-level understanding of the relationships between glass composition, structure, and solubility, and optimization of the dissolution rate of these glasses for specific biomedical applications is currently limited to trial-and-error approaches.

There have only been very few atomistic simulations of phosphate-based glasses in the P_2O_5−CaO−Na_2O system, and they are mostly limited to short-range (radial and angular distribution functions) and medium-range (Q^n distributions and network connectivity) properties.[10,11] Changes in the Q^n distribution, where n is the number of bridging oxygen (BO) atoms (oxygen atoms that link two phosphorus atoms) per PO_4 tetrahedron, and in the network connectivity (the mean value of n), strongly affect the solubility of the glass networks.[12] But the network connectivity depends only on the ratio of the numbers of oxygen and phosphorus atoms,[13,14] which does not change with Ca versus Na substitution. The profound changes in the observed dissolution rate as a result of changing Na and Ca content therefore must have another cause.

Here we show, using molecular dynamics simulations, that the calcium atoms cross-link more fragments of the phosphate glass network than the sodium atoms do, which enhances the durability of the glass. Further, we show that this increased cross-linking is a direct result of calcium's higher field strength and associated preference for binding to nonbridging oxygen atoms. This molecular-level insight offers a predictive, computer-aided route to the precise control of the dissolution rate of these glasses in a physiological environment, and hence their optimization for diverse biomedical applications.

METHODS

We have used the DL_POLY program[15] to conduct classical molecular dynamics (MD) simulations of different compositions of ternary PBG, using a methodology and force field known to produce reliable structural models of glasses,[16,17] including phosphate glass.[11] About 3000 atoms in the right composition are placed at random (subject to being not unphysically close) in a cubic periodic box at the experimental room-temperature density. The exact densities, numbers of

Received: June 12, 2013
Revised: August 9, 2013
Published: August 15, 2013

atoms, and box sizes are given in Table 1. The box is equilibrated for 200 ps in an NVT ensemble at 2500 K, and

Table 1. Densities (ρ), Numbers of Atoms (N), and Box Sizes Studied

composition	ρ (g/cm^3)	N	box size (Å)
C25	2.55	3003	34.61
C30	2.56	3001	34.65
C35	2.57	2998	34.69
C40	2.59	3001	34.71
C45	2.60	3006	34.78

then cooled through several NVT ensembles at an overall cooling rate of 5.5 K/ps; this cooling rate is of the same order of magnitude as previous simulations which have given structures in agreement with experiment.[11,16,18,19] They are then equilibrated at 300 K for 50 ps, and all data quoted here are averaged over a subsequent 150 ps production run in an NVT ensemble at 300 K.

The force field was previously developed by us[11] and assumes that interactions between atoms i and j are given by a Buckingham potential combined with the electrostatic Coulomb interactions as follows

$$V_{ij}(r_{ij}) = A_{ij}\exp\left(-\frac{r_{ij}}{\rho_{ij}}\right) - \frac{C_{ij}}{r_{ij}^6} + \frac{q_i q_j}{r_{ij}} \quad (1)$$

where A_{ij}, ρ_{ij}, and C_{ij} are the Buckingham potential parameters for interactions between atoms i and j, r_{ij} is the interatomic distance between atoms i and j, and q_i is the charge of atom i, which are the formal ionic charges. Polarizability is included in the oxygen atoms only by splitting its charge between a core of charge +0.8482e and a shell of charge −2.8482e, which are coupled by a harmonic spring with spring constant 74.92 eV Å^{-2}. The Ewald summation[20] is used to evaluate the contribution of the Coulomb forces. Three-body interactions are included through a harmonic potential $V(\theta) = (1/2)k_{3b}(\theta - \theta_0)^2$, where k_{3b} is the three-body spring constant, θ the bond angle, and θ_0 a potential parameter. The full potential parameters are given in Table 2.

Table 2. Force-Field Parameters Used

	$A\exp(-r/\rho) - Cr^{-6}$		
	A (eV)	ρ (Å)	C (eV Å^6)
P−O$_s$	1020.0	0.34322	0.03
O$_s$−O$_s$	22764.3	0.149	27.88
Na−O$_s$	56465.3453	0.193931	0.0
Ca−O$_s$	2152.3566	0.309227	0.09944
	$(1/2)k_{3b}(\theta - \theta_0)^2$		
	k_{3b} (eV rad^{-2})	θ_0 (deg)	
O$_s$−P−O$_s$	3.3588	109.47	
P−O$_s$−P	7.6346	141.1793	

Although the cooling rate used to prepare these glasses is several orders of magnitude faster than that used to prepare glasses experimentally, the methodology used here does not lead to significant differences from experiment in the atomic structure. In our previous work[11] which introduced the phosphate force field, the same cooling rate and methodology were used to prepare some of the same compositions. In that work, the structures of the glasses were extensively compared against available experimental data, including neutron and X-ray diffraction and solid-state NMR spectra, with which they were found to be in good agreement. Our cooling rate is also lower than those used normally to converge reliable glass structures.[16,18,19]

Density-functional theory (DFT) calculations were performed using the Perdew−Burke−Ernzerhof (PBE)[21] exchange-correlation functional and the DMol^3 code.[22] DMol^3 implements DFT using localized atom-centered numerical orbitals. We have used the all-electron double-numeric-polarized (DNP) basis sets on all atoms, which is variationally comparable to the 6-31G(d,p) Gaussian basis set, but the numerical functionals are far more complete than the traditional Gaussian functions. Owing to the quality of these orbitals, basis set superposition effects are minimized, weak bonds are very well described, and it has been shown that the methodology used in this work provides accurate energies of formation for calcium−oxygen type of complexes.[23] Each basis function was restricted to a large cutoff radius of 6.5 Å in order to describe properly the diffuse nature of the wave function of the phosphate anions. The electron density was approximated using a multipolar expansion up to octopole.

RESULTS AND DISCUSSION

We have studied five ternary phosphate-based glasses consisting of 45 mol % P_2O_5, 25−45 mol % CaO, and the remainder of the glass made up of Na_2O. The glasses will be referred to as, for example, C30, for the composition with 30 mol % CaO. The changes in dissolution rate are profound even for small changes in composition in this range; Ahmed et al.[3] found that the solubility of the C30 composition in water is 1.3×10^{-3} mg cm^{-2} h^{-1}, compared to 2.0×10^{-4} mg cm^{-2} h^{-1} for the C35 composition, and 1.6×10^{-4} mg cm^{-2} h^{-1} for the C40 composition.

At these compositions, the network connectivity is about 1.8, and the basic structure of these glasses is known from theory,[14] experimental observations,[1,3] and simulations[11] to consist of short chains of connected phosphate PO_4 tetrahedra, without rings and only very few branches. Hence, the phosphorus atoms for these compositions are mostly Q^2 with (almost all of) the rest being Q^1. (Our simulations find a small amount, typically about 5%, of Q^3 phosphorus atoms.) The average chain length depends only on the ratio of the numbers of oxygen and phosphorus atoms,[13,14] which is constant for these compositions, and indeed our simulated values of the average chain lengths are almost constant too. The distributions of chain lengths observed are shown in Figure 1, which shows very little variation between different compositions, and no trend as a function of Na/Ca ratios, reflecting the very small changes in the Q^n distributions for these compositions.[11]

A variety of phosphate glasses around the metaphosphate composition are seen to dissolve uniformly,[24,25] such that the ionic concentration of the glass dissolution products in solution is the same as the glass composition. A comparison of the phosphate chain lengths in the glass and in solution shows that the dominant way these glasses dissolve is by hydrating entire phosphate chains intact into solution, with any subsequent hydrolysis only occurring over much longer time scales.[26] Also, the length and structure of the chains, and the network connectivity, do not change with varying glass composition. Since the chains are not altered during the dissolution process, and their structure does not depend on composition, the

dx.doi.org/10.1021/jp4058115 | J. Phys. Chem. B 2013, 117, 10652−10657

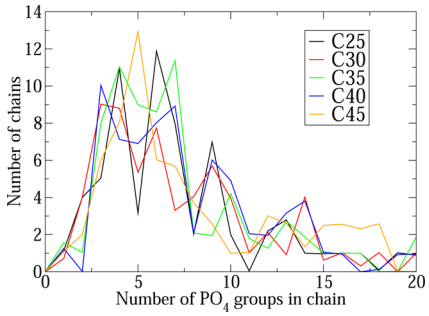

Figure 1. Distributions of the phosphate chain lengths in the different compositions. The mean chain lengths are 8.5 (composition C25), 8.6 (C30), 8.0 (C35), 8.4 (C40), and 8.7 (C45) phosphate units.

observed changes in the glass dissolution rate must therefore reflect differences in how the phosphate chains are bound to the rest of the glass structure.

In particular, it has often been suggested[24,27−30] that the Ca^{2+} ion adopts a chelating structure in these glasses, shown schematically in Figure 2, bonding through its neighboring

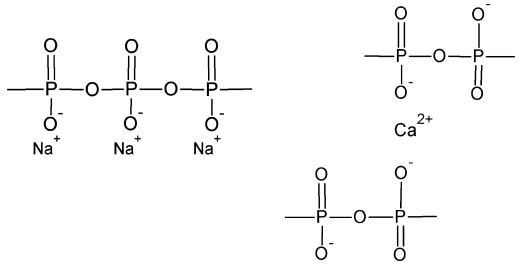

Figure 2. A schematic of an often-suggested difference between the bonding of Na and Ca in phosphate glasses. This paper shows that this picture is, at best, a substantial oversimplification.

oxygen atoms to different chains of the phosphate glass network and thus holding the network together and making it more resistant to dissolution in a way that the Na^+ ion does not. Previous works[4,24] have used charge-balancing arguments to propose that Ca^{2+} binds to two nonbridging oxygen (NBO) atoms (which can be on separate chains, as shown in Figure 2), and Na^+ only binds to one, implying that Na^+ cannot cross-link different chains.

However, these arguments do not take into account the structure of these glasses known from spectroscopic and diffraction experiments,[13,14,31,32] which show that both Na and Ca coordinate to large numbers of oxygen atoms (∼ 5−8, depending on composition and type of glass), rather than only one or two. Also, simulated results reported elsewhere[11] show that the nearest-neighbor atomic environments of Na and Ca are actually rather similar for these compositions; both act as network modifiers, with modifier−oxygen bond lengths of about 2.3 Å, and with high oxygen coordination numbers (both BO and NBO), i.e., 6.4−6.8 for Na and 6.6−6.8 for Ca. Almost all of the atoms in the first coordination shell of both Na and Ca are known to be NBOs, although the difference in this number between the two cation coordination shells is, in fact, crucial to understanding the dissolution behavior, as we discuss later.

Although the proposed chelating structures were not found, we do observe a substantial difference between the ability of Na and Ca to cross-link different phosphate chains. We have identified all of the chains in our models and introduced a new protocol to characterize the environment of the network-modifying cations, namely by computing their ability to anchor simultaneously a number of phosphate chains. We then note that, on average, a Ca atom is bonded to 3.9−4.0 chains, while a Na atom is only bonded to 3.2−3.3 chains, a significant difference in behavior which has not been identified previously, and is inaccessible by experiment. This difference in the numbers of chains bonded to the different modifier ions means that increasing the Ca content and decreasing the Na content will mean that more chains are bound together through a modifier atom, thereby strengthening the glass network and leading to the experimentally observed lower dissolution rates. The full distribution of number of chains bound to modifiers is shown in Table 3, and a representative example of a Na atom bound to three phosphate fragments is shown in Figure 3.

Table 3. Percentage Distribution of Number of Phosphate Chains Bonded to Na and Ca

	Na (%)							
	0	1	2	3	4	5	6	average
C25	0.0	1.2	15.4	46.3	32.0	4.4	0.6	3.25
C30	0.0	1.8	9.9	52.7	32.3	3.3	0.0	3.25
C35	0.0	0.4	14.9	46.6	32.3	5.6	0.2	3.28
C40	0.0	1.0	14.1	48.8	32.2	3.7	0.3	3.24
C45	0.0	1.3	17.9	44.8	29.9	6.1	0.0	3.22
	Ca (%)							
	0	1	2	3	4	5	6	average
C25	0.0	0.0	3.1	23.9	47.7	21.9	2.7	3.95
C30	0.0	0.0	5.0	31.2	40.9	20.0	2.9	3.85
C35	0.0	0.0	5.7	22.2	45.3	24.4	2.5	3.96
C40	0.0	0.0	3.7	24.7	50.6	17.6	3.3	3.92
C45	0.0	0.0	4.5	24.9	48.5	20.0	2.1	3.90

The different bonding behavior of the two modifier atoms is caused by the fact that calcium has a higher charge, and a higher field strength, than sodium. While all modifier atoms prefer to bond to nonbridging oxygen (NBO) atoms instead of bridging oxygen (BO) atoms, if two modifiers are present then the coordination environment of the atom with the higher field strength is satisfied at the expense of that of the atom with the lower field strength.[33] The Dietzel definition of field strength F is $F = Z/a^2$, where Z is the modifier ion charge and a is the modifier−oxygen bond length in an octahedral environment.[34] Since a is roughly similar for both Na and Ca in these compositions, the difference in charge between the Na^+ and Ca^{2+} ions accounts for the different bonding behavior. Indeed, for these compositions, we observed that Ca has 6.1−6.2 NBO neighbors, compared to Na, which has 5.2−5.4.[11] An NBO will prefer to bond to the higher-charged Ca atom. Na will therefore have more BO atoms in its coordination shell, which, by definition, are bonded to two phosphorus atoms that are part of the same chain. This will reduce the number of chains bound to Na, either by making more of Na's first coordination shell part of the same chain or by sterically restricting the space available for more chains to coordinate to the Na. Ca's preference for NBO in its first coordination shell will therefore lead to more chains surrounding Ca than Na, as observed. We note also that the idea that Na bonds only to one NBO, or Ca to two NBOs, is quite false.

dx.doi.org/10.1021/jp4058115 | J. Phys. Chem. B 2013, 117, 10652−10657

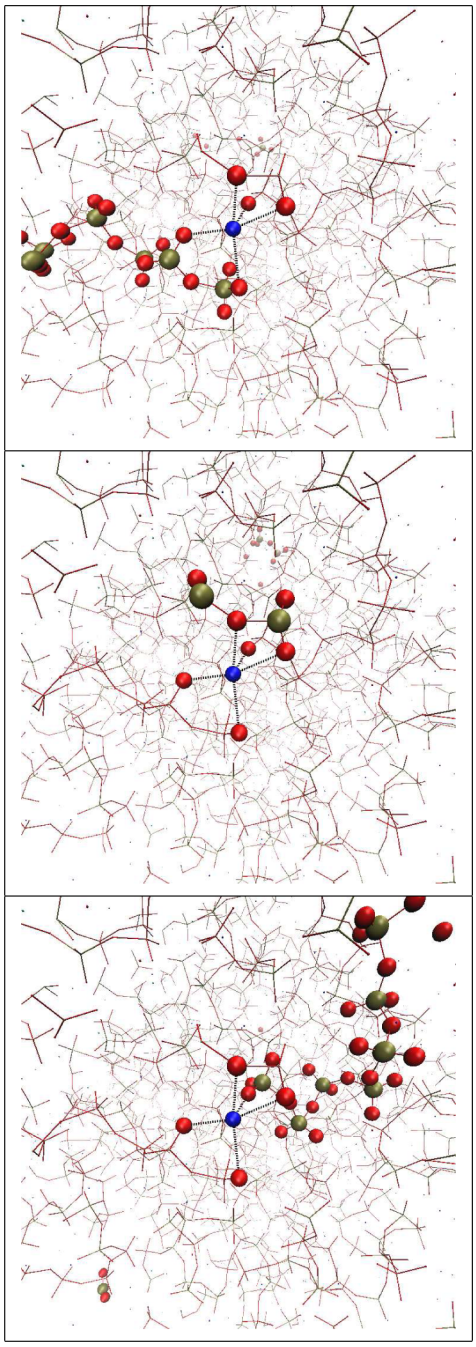

Figure 3. A Na atom bound to three phosphate fragments. The central Na atom (blue) and its first coordination shell are highlighted in all pictures; each picture highlights a different phosphate fragment anchored to the Na. The remainder of the glass structure has been shrunk for clarity.

Although the location and bonding of the phosphate chains themselves control the dissolution, the differences we observe will also be reflected elsewhere in the glass structure, in features which may be easier to observe in experiment, through e.g., solid-state NMR spectroscopy. We have therefore computed some additional relevant structural features at the same length scale, which also reflect the difference in dissolution rates. We have measured the number of PO_4 tetrahedra bonded to the modifier ions, by computing the number of distinct phosphorus atoms bonded to oxygen atoms in the first coordination shell of each of the modifier atoms. This will of course reflect Ca's superior ability over Na to bond to NBOs, as well as differences in the distribution of chains around the cations. We found that Na is bonded to 5.8−6.0 PO_4 tetrahedra, while Ca is bonded to 6.3−6.4. Again, this shows that Ca binds together more tetrahedra than Na, which would intuitively lead to a stronger network that is less prone to dissolution.

In silicate-based glasses, differences have been observed in the amount of so-called "intratetrahedral" bonding around different modifiers.[19,35] Intratetrahedral bonding is the phenomenon by which a PO_4 (or SiO_4) tetrahedron bonds to a given modifer through two of its oxygen atoms rather than one. Increased intratetrahedral bonding is likely to decrease the number of distinct PO_4 tetrahedra—and the number of phosphate chains—bound together by a single modifier, and hence weaken the network. We found that an average Na atom had 1.2−1.3 intratetrahedral bonds, while Ca had only 0.9−1.1 (Table 4, n = 1). Previous work[11] has identified that Na has a broader bond-angle distribution than Ca and is thus more likely to adopt the bidentate bonding necessary for two of its oxygen neighbors to belong to the same phosphate tetrahedron. Ca's smaller propensity for intratetrahedral bonding is likely to contribute strongly to the higher number of PO_4 tetrahedra found around a Ca atom, and hence its strengthening effect on the network. We have also computed the prevalence of different $(O-P-)_n-O$ chain lengths around Na and Ca, where the two terminal oxygen atoms are bonded to the same modifier; i.e., the modifier "closes" the ring structure and the results are shown in Table 4. Shorter chains are more numerous around both modifiers, and the differences between compositions are negligible. We also note the average number of $(O-P-)_2-O$ and $(O-P-)_3-O$ chains around Na increases steadily and significantly with increasing Ca content across all compositions studied.

Table 4. Average Number of M···$(O-P-)_n$−O···M Chains of Length n around a Single M Atom, Where M = Na or Ca

	n	C25	C30	C35	C40	C45
Na	1	1.21	1.20	1.25	1.22	1.26
	2	0.77	0.78	0.88	0.91	0.88
	3	0.44	0.47	0.54	0.56	0.67
Ca	1	0.91	1.10	0.97	0.89	0.91
	2	0.88	0.89	0.80	0.83	0.90
	3	0.51	0.52	0.60	0.66	0.53

We have shown that characterizing the modifier−phosphate-chain bonding is crucial to understanding the glass dissolution behavior. We now show that the distribution of phosphate chain formation can be characterized through the use of accurate density-functional theory simulations, and that the populations of the various chain lengths can be understood through considering the energies of formation of sodium and calcium complexes with phosphate chains of different lengths.

These energies of formation ($\Delta E_e = \sum_{products} E_e - \sum_{reactants} E_e$) provide information about the relative configurational stabilities of each complex in the gas phase, in terms of the total electronic energy change at 0 K. The complexes containing a phosphorus chain with two phosphate groups have more negative ΔE_e values (ΔE_e for $Na(H_2PO_4)_2^- + H_2P_2O_7^{2-} \rightarrow Na(H_2PO_4)(H_2P_2O_7)^{2-} + H_2PO_4^-$ = −32.54 kcal mol^{-1}, and −103.57 kcal mol^{-1} for the equivalent Ca reaction) than the corresponding three-membered phosphate chains for like cations (−12.47 and −93.18 kcal mol^{-1}, respectively). (The

dx.doi.org/10.1021/jp4058115 | J. Phys. Chem. B 2013, 117, 10652−10657

hydrogen atoms are included to charge balance the oxygen atoms not bonded to the modifier.) This increased stability partly explains the increased number of two-membered (n = 2) chains compared with three-membered (n = 3) chains for both sodium and calcium across all three compositions studied (Table 4).

CONCLUSION

To conclude, we have shown that the experimentally observed decrease in solubility of ternary phosphate-based bioglasses when the calcium content is raised is more complex than originally envisaged. It is caused by Ca binding together more phosphate chains than Na, which is rooted in Ca's higher field strength, which means that Ca can satisfy its bonding preference for nonbridging oxygen neighbors at the expense of Na. In addition to binding together more phosphate chains, we confirm that Ca bonds to more PO_4 tetrahedra and has a lower concentration of intratetrahedral phosphate bonding than Na, both features which will enhance the glass's durability as more Ca is included. Ca also has an increased energetic favorability for longer chains bound around it than Na, which is confirmed by accurate density-functional calculations. This increased understanding of the structural factors which control the glass dissolution rate will help to optimize glass compositions for very specific biomedical applications, e.g., as the carriers for the controlled release of drugs or antimicrobial agents.

AUTHOR INFORMATION

Corresponding Author

*E-mail: jamieson.christie@ucl.ac.uk.

Notes

The authors declare no competing financial interest.

ACKNOWLEDGMENTS

We are grateful to the EPSRC and the Royal Society for research funding. Via our membership of the UK's HPC Materials Chemistry Consortium, which is funded by EPSRC (EP/F067496), this work made use of the facilities of HECToR, the UK's national high-performance computing service. The authors acknowledge the use of the UCL Legion High Performance Computing Facility (Legion@UCL), and associated support services, in the completion of this work.

REFERENCES

(1) Abou Neel, E. A.; Pickup, D. M.; Valappil, S. P.; Newport, R. J.; Knowles, J. C. Bioactive Functional Materials: a Perspective on Phosphate-based Glasses. *J. Mater. Chem.* **2009**, *19*, 690−701.

(2) Gilchrist, T.; Glasby, M. A.; Healy, D. M.; Kelly, G.; Lenihan, D. V.; McDowall, K. L.; Miller, I. A.; Myles, L. M. In vitro Nerve Repair - in vivo. The Reconstruction of Peripheral Nerves by Entubulation with Biodegradable Glass Tubes - a Preliminary Report. *Br. J. Plas. Surg.* **1998**, *51*, 231−237.

(3) Ahmed, I.; Lewis, M.; Olsen, I.; Knowles, J. C. Phosphate Glasses for Tissue Engineering: Part 1. Processing and Characterisation of a Ternary-based P_2O_5-CaO-Na_2O Glass System. *Biomaterials* **2004**, *25*, 491−499.

(4) Uo, M.; Mizuno, M.; Kuboki, Y.; Makishima, A.; Watari, F. Properties and Cytotoxicity of Water Soluble Na_2O-CaO-P_2O5 Glasses. *Biomaterials* **1998**, *19*, 2277−2284.

(5) Valappil, S. P.; Pickup, D. M.; Carroll, D. L.; Hope, C. K.; Pratten, J.; Newport, R. J.; Smith, M. E.; Wilson, M.; Knowles, J. C. Effect of Silver Content on the Structure and Antibacterial Activity of Silver-doped Phosphate-based Glasses. *Antimicrob. Agents Deliv.* **2007**, *51*, 4453−4461.

(6) Pickup, D. M.; Newport, R. J.; Knowles, J. C. Sol-gel Phosphate-based Glass for Drug Delivery Applications. *J. Biomater. Appl.* **2012**, *26*, 613−622.

(7) Knowles, J. C. Phosphate Based Glasses for Biomedical Applications. *J. Mater. Chem.* **2003**, *13*, 2395−2401.

(8) Franks, K.; Abrahams, I.; Knowles, J. C. Development of Soluble Glasses for Biomedical Use Part I: in vitro Solubility Measurement. *J. Mater. Sci.: Mater. Med.* **2000**, *11*, 609−614.

(9) Knowles, J. C.; Franks, K.; Abrahams, I. Investigation of the Solubility and Ion Release in the Glass System K_2O-Na_2O-CaO-P_2O_5. *Biomaterials* **2001**, *22*, 3091−3096.

(10) Tang, E.; Di Tommaso, D.; de Leeuw, N. H. An ab initio Molecular Dynamics Study of Bioactive Phosphate Glasses. *Adv. Eng. Mater.* **2010**, *12*, B331−B338.

(11) Ainsworth, R. I.; Di Tommaso, D.; Christie, J. K.; de Leeuw, N. H. Polarizable Force Field Development and Molecular Dynamics Study of Phosphate-based Glasses. *J. Chem. Phys.* **2012**, 137.

(12) Tilocca, A. Structural Models of Bioactive Glasses from Molecular Dynamics Simulations. *Proc. R. Soc. A* **2009**, *465*, 1003−1027.

(13) Brow, R. K. Review: the Structure of Simple Phosphate Glasses. *J. Non-Cryst. Solids* **2000**, *263&264*, 1−28.

(14) Hoppe, U. A Structural Model for Phosphate Glasses. *J. Non-Cryst. Solids* **1996**, *195*, 138−147.

(15) Todorov, I. T.; Smith, W.; Trachenko, K.; Dove, M. T. DL POLY 3: New Dimensions in Molecular Dynamics Simulations via Massive Parallelism. *J. Mater. Chem.* **2006**, *16*, 1911−1918.

(16) Tilocca, A.; Cormack, A. N.; de Leeuw, N. H. The Structure of Bioactive Silicate Glasses: New Insight from Molecular Dynamics Simulations. *Chem. Mater.* **2007**, *19*, 95−103.

(17) Christie, J. K.; Tilocca, A. Aluminosilicate Glasses as Yttrium Vectors for in situ Radiotherapy: Understanding Composition-Durability Effects through Molecular Dynamics Simulations. *Chem. Mater.* **2010**, *22*, 3725−3734.

(18) Vollmayr, K.; Kob, W.; Binder, K. Cooling-rate Effects in Amorphous Silica: A Computer-Simulation Study. *Phys. Rev. B* **1996**, *54*, 15808−15827.

(19) Christie, J. K.; Malik, J.; Tilocca, A. Bioactive Glasses as Potential Radioisotope Vectors for in situ Cancer Therapy: Investigating the Structural Effects of Yttrium. *Phys. Chem. Chem. Phys.* **2011**, *13*, 17749−17755.

(20) Ewald, P. P. Die Berechnung Optishcer und Elektrostatischer Gitterpotentiale. *Ann. Phys.* **1921**, *369*, 253−287.

(21) Perdew, J. P.; Burke, K.; Ernzerhof, M. Generalized Gradient Approximation Made Simple. *Phys. Rev. Lett.* **1996**, *77*, 3865−3868.

(22) Delley, B. From Molecules to Solids with the DMol3 Approach. *J. Chem. Phys.* **2000**, *113*, 7756−7764.

(23) Di Tommaso, D.; de Leeuw, N. H. The Onset of Calcium Carbonate Nucleation: A Density Functional Theory Molecular Dynamics and Hybrid Microsolvation/Continuum Study. *J. Phys. Chem. B* **2008**, *112*, 6965−6975.

(24) Bunker, B. C.; Arnold, G. W.; Wilder, J. A. Phosphate Glass Dissolution in Aqueous Solutions. *J. Non-Cryst. Solids* **1984**, *64*, 291−316.

(25) Brow, R. K. The Nature of Alumina in Phosphate Glass I. Properties of Sodium Aluminophosphate Glass. *J. Am. Ceram. Soc.* **1993**, *76*, 913−918.

(26) Brauer, D. S. *Bio-Glasses: An Introduction*; Wiley: New York, 2012; Chapter 4.

(27) vanWazer, J. R.; Holst, K. A. Structure and Properties of the Condensed Phosphates. I. Some General Considerations about Phosphoric Acids. *J. Am. Chem. Soc.* **1950**, *72*, 639−644.

(28) van Wazer, J. R.; Campanella, D. A. Structure and Properties of the Condensed Phosphates. IV. Complex Ion Formation in Polyphosphate Solutions. *J. Am. Chem. Soc.* **1950**, *72*, 655−663.

(29) Gao, H.; Tan, T.; Wang, D. Effect of Composition on the Release Kinetics of Phosphate Controlled Release Glasses in Aqueous Medium. *J. Controlled Release* **2004**, *96*, 21−28.
(30) Gao, H.; Tan, T.; Wang, D. Dissolution Mechanism and Release Kinetics of Phosphate Controlled Release Glasses in Aqueous Medium. *J. Controlled Release* **2004**, *96*, 29−36.
(31) Hoppe, U.; Walter, G.; Kranold, R.; Stachel, D. Structural Specifics of Phosphate Glasses Probed by Diffraction Methods: a Review. *J. Non-Cryst. Solids* **2000**, *263&264*, 29−47.
(32) Strojek, W.; Eckert, H. Medium-range Order in Sodium Phosphate Glasses: a Quantitative Rotational Echo Double Resonance Solid State NMR Study. *Phys. Chem. Chem. Phys.* **2006**, *8*, 2276−2285.
(33) Varshneya, A. K. *Fundamentals of Inorganic Glasses*; Academic Press: New York, 1993.
(34) Dietzel, A. *Z. Electrochem.* **1942**, *48*, 9−23.
(35) Christie, J. K.; Tilocca, A. Integrating Biological Activity into Radioisotope Vectors: Molecular Dynamics Models of Yttrium-Doped Bioactive Glasses. *J. Mater. Chem.* **2012**, *22*, 12023−12031.